

INTRODUCTION

Examinations of functional connectivity (FC) changes over time are becoming a significant focus in human neuroimaging studies [1], but these dynamics can be difficult to understand and validate [2,3]. Using simultaneously acquired optical recordings of neural and hemodynamic data in awake mice, we examine how connectivity changes across the cortical surface across repeated measurements.

The data presented here are from two Thy1-GCaMP6f mice with 36 three minute imaging sessions over three days. For each mouse, we created regions of interest and calculated correlations between all pairs of regions across time. Using these data, we examined the stability of connections based on GCaMP fluorescence, total hemoglobin (HbT) and deoxyhemoglobin (HbR) across time. We also were able to compare the connectivity profiles across modalities to examine the strength and stability of the connectivity relationship between GCaMP and HbT or HbR.

METHODS

Data Acquisition and Preprocessing

Handling and Running Wheel Habituation

Thy1-GCaMP6f mice (Jackson Laboratory, Stock #025393) were weaned in cages with a Fast-Trac running wheel mounted on Mouse Igloos (Bio-Serv) and handled 3-5 times weekly with treats until habituated to human handling and running wheel.

Preparation

Adult mice were anesthetized with isoflurane and underwent thinned-skull craniotomy over the cortex between coronal and lambdaoid sutures, and implanted with an acrylic headpiece for restraint.

The thinned-skull craniotomy is protected by an optically clear cyanoacrylate layer (applied during surgery) and Kwik-Sil (WPI) silicone (to be removed and reapplied between each imaging session).

After a two-day post-operative recovery period, imaging sessions were conducted with awake restrained mice running or resting on a Fast-Trac wheel or custom-made acrylic wheel with webcam monitoring beneath.

Wide Field Optical Mapping (WFOM) [6]

Sequentially strobing high-powered LEDs at three different wavelengths: 490, 530, and 625 nm

780 nm IR LED used for webcam illumination

500-650 nm band pass emission filter

High-speed EMCCD (Andor) iXon camera time-locked with LEDs

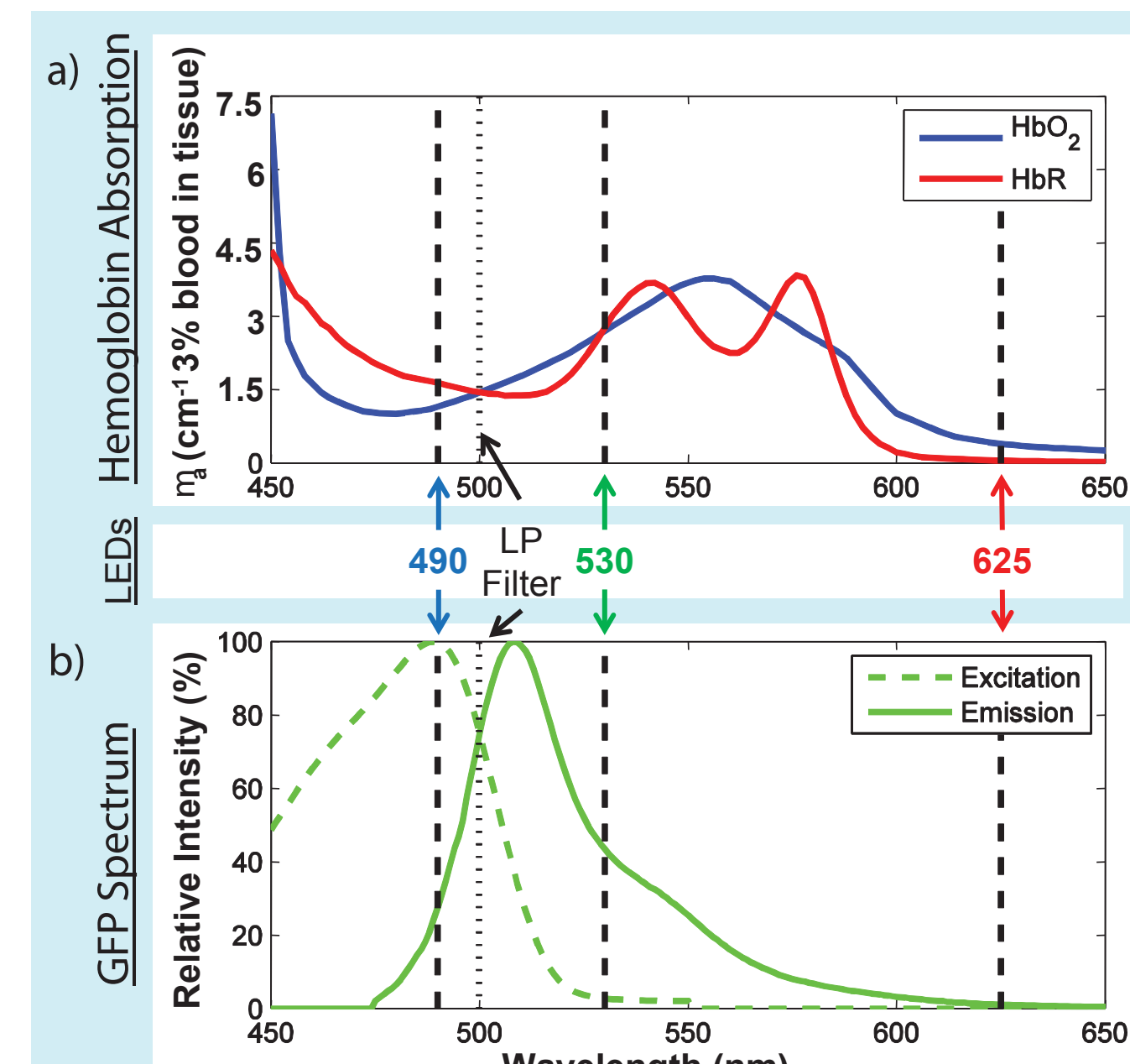
Images can be acquired faster than 100 frames per second at greater than 1 megapixel resolution

Data Acquisition and Pre-Processing

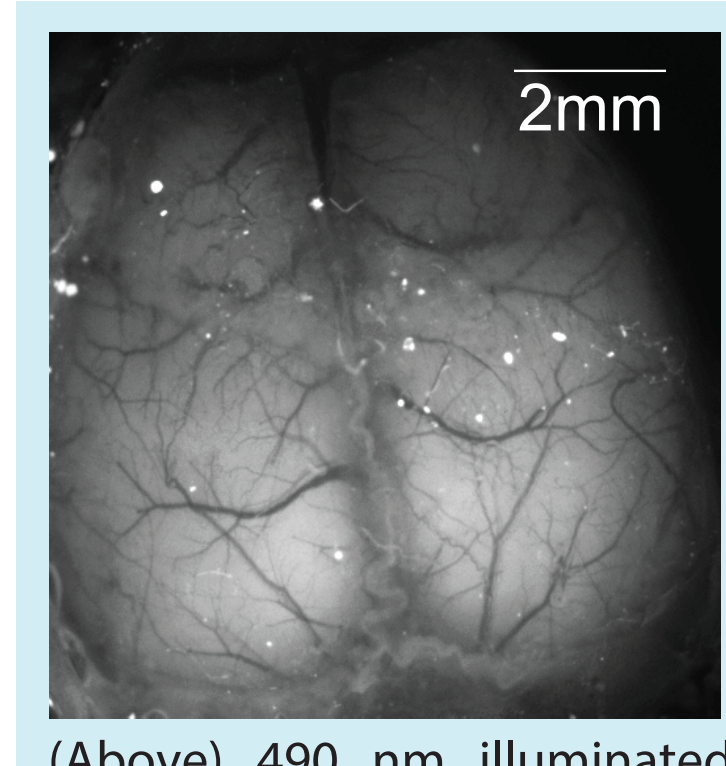
31 frames per second / 30 ms exposure

Oxy-hemoglobin (HbO₂), deoxy-hemoglobin (HbR), and total hemoglobin (HbT) data converted from red and green channels using hemoglobin spectra. Blue channel converted to GCaMP6 fluorescence (hemodynamic signal regressed using Monte Carlo-based correction [7]).

Image registration and moving average filter of 3 frames used to remove motion artifacts.

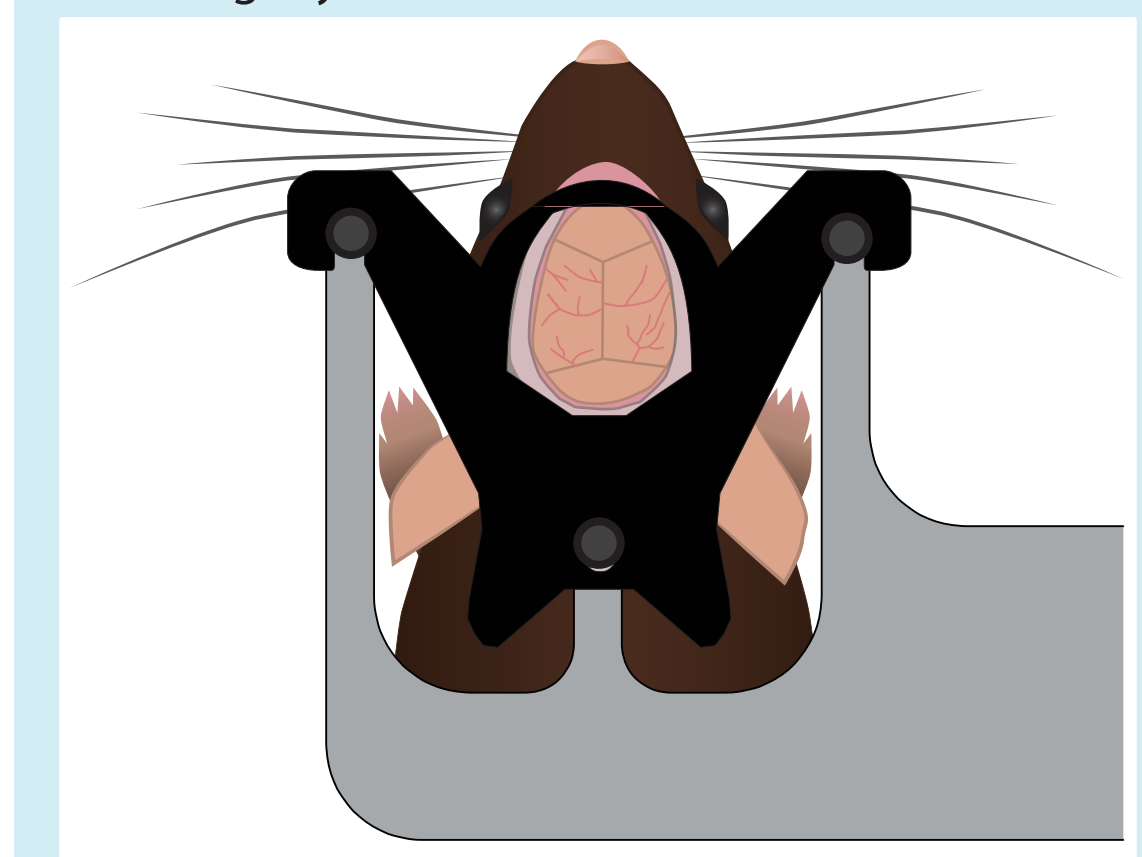


(a) Differences in hemoglobin absorption spectra and strategically chosen LED wavelengths allow quantification of oxy-hemoglobin (HbO₂), deoxy-hemoglobin (HbR), and total hemoglobin (HbT) concentration changes [4].
(b) Excitation and emission spectra of GFP, genetically encoded and expressed in layer II/III and V neurons in Thy1-GCaMP6f mouse cortex [5].



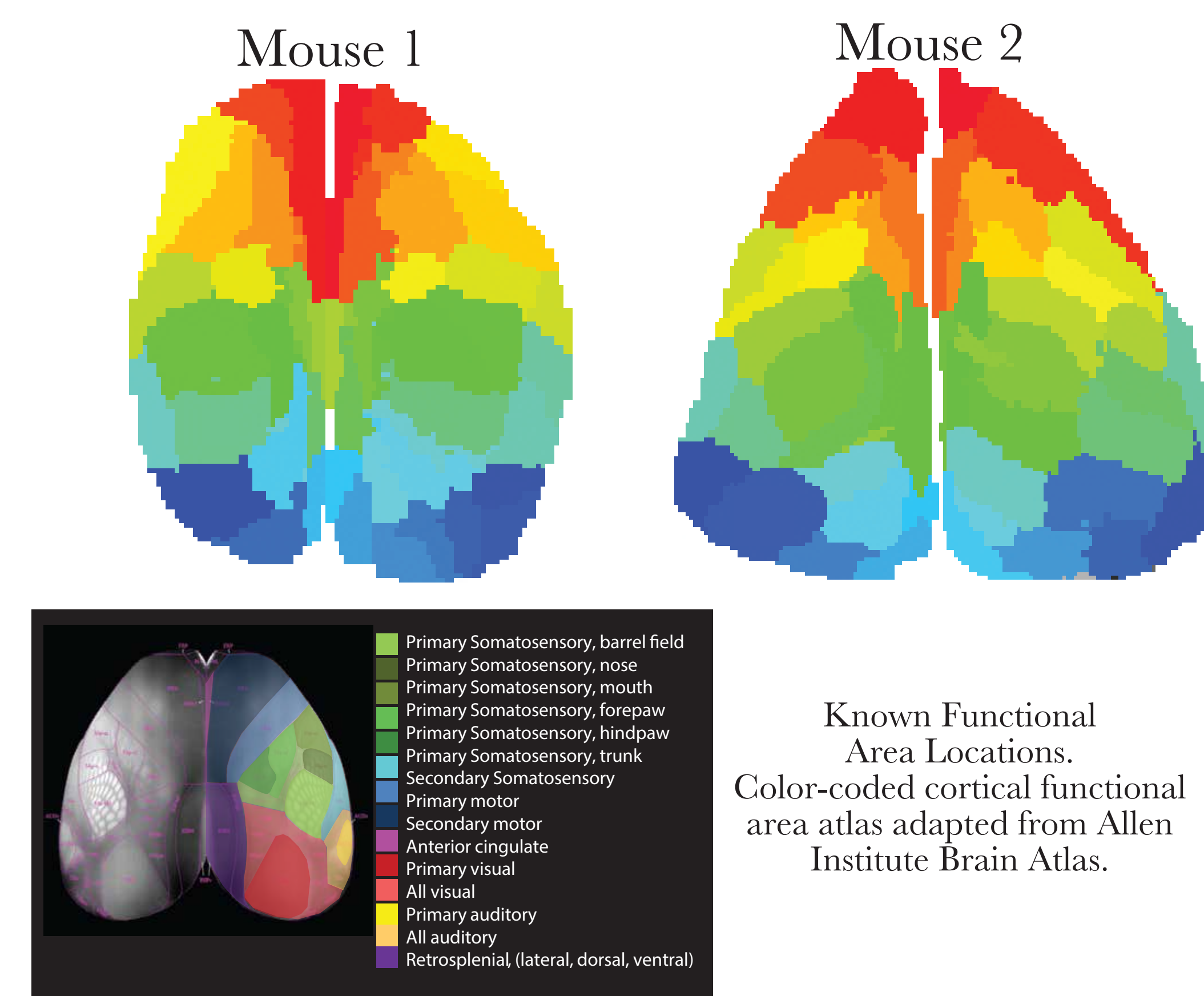
(Left) Awake mouse imaging rig hardware

(Below) This acrylic head plate held with screws onto an aluminum holder allows for maximized cortical visibility while holding the head rigidly to eliminate most motion artifact.



CONNECTIVITY ANALYSIS METHODS

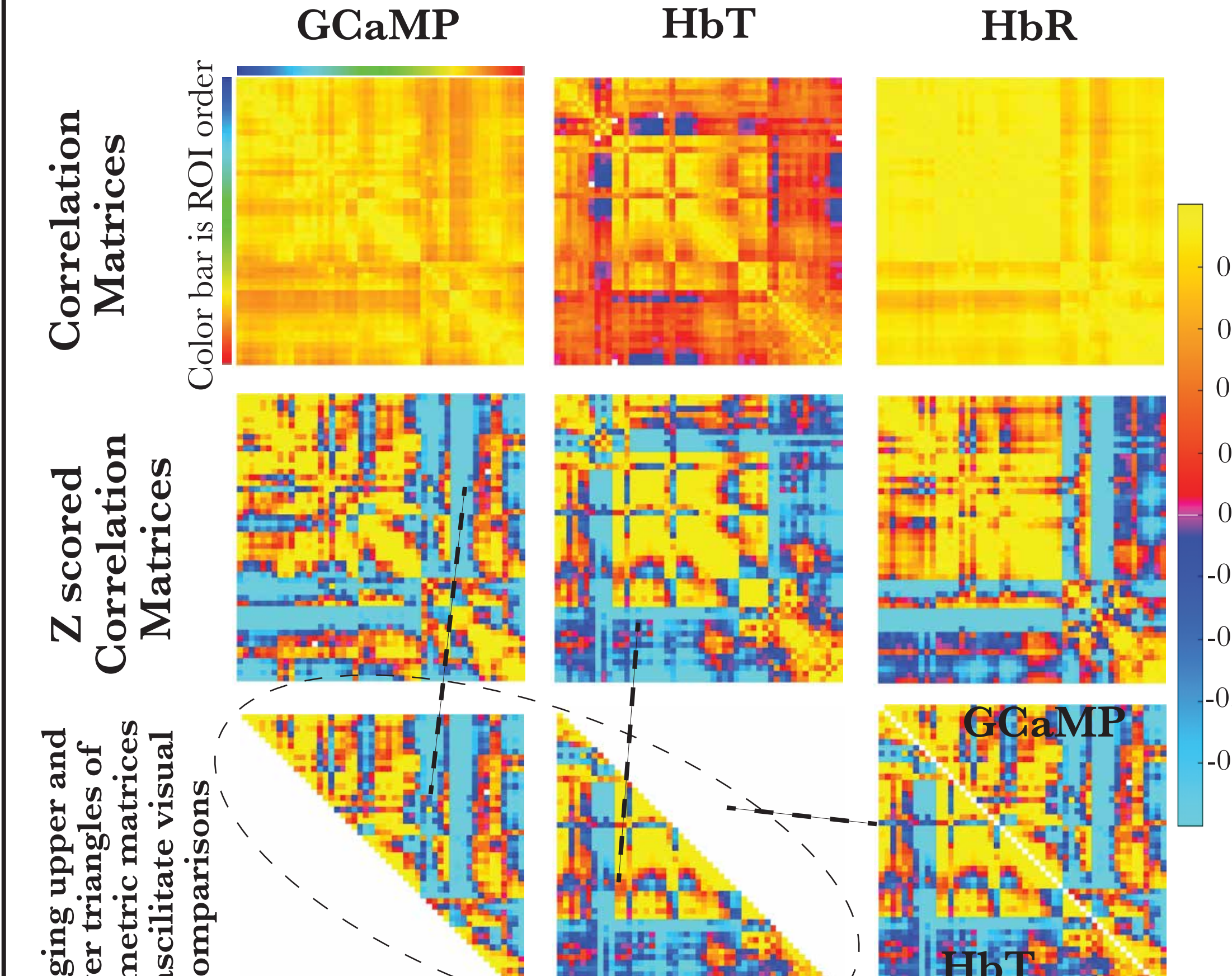
Regions of interest for each mouse



Known Functional Area Locations. Color-coded cortical functional area atlas adapted from Allen Institute Brain Atlas.

A mask of the exposed cortical surface was made for each mouse. K-means clustering using Pearson correlation as a distance measure was applied to GCaMP and HbT data concatenated across all runs. Low frequency signal drifts were removed and frames where the mice's legs were visibly moving were removed. The mean ROI time series from each 3 min run were correlated. The ROIs are ordered spatially from caudal to rostral so that the correlation matrices reflected the spatial structure of the brain. 3 runs from mouse 2 were excluded because the mouse was moving more than half the run.

Correlation Matrices



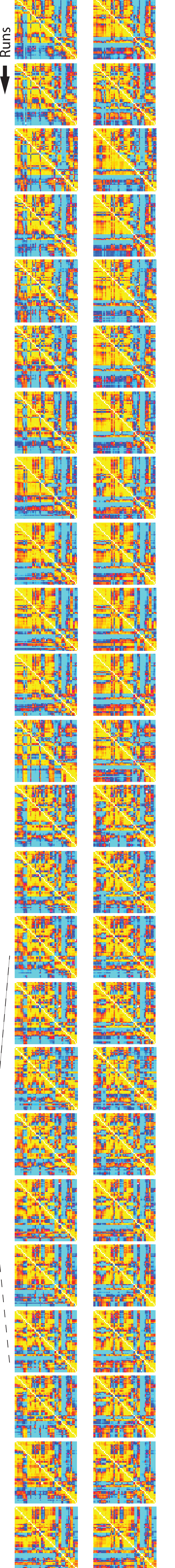
Correlation Matrices from a sample 3 minute run. The first row is scaled by r value, but structural similarities and differences in the connectivity patterns are obscured by baseline or magnitude shifts. The second row is mean centered and standard deviation normalized. The matrices that combine triangles for GCaMP (upper left) and Hb (lower right) are shown across 24 runs.

REFERENCES

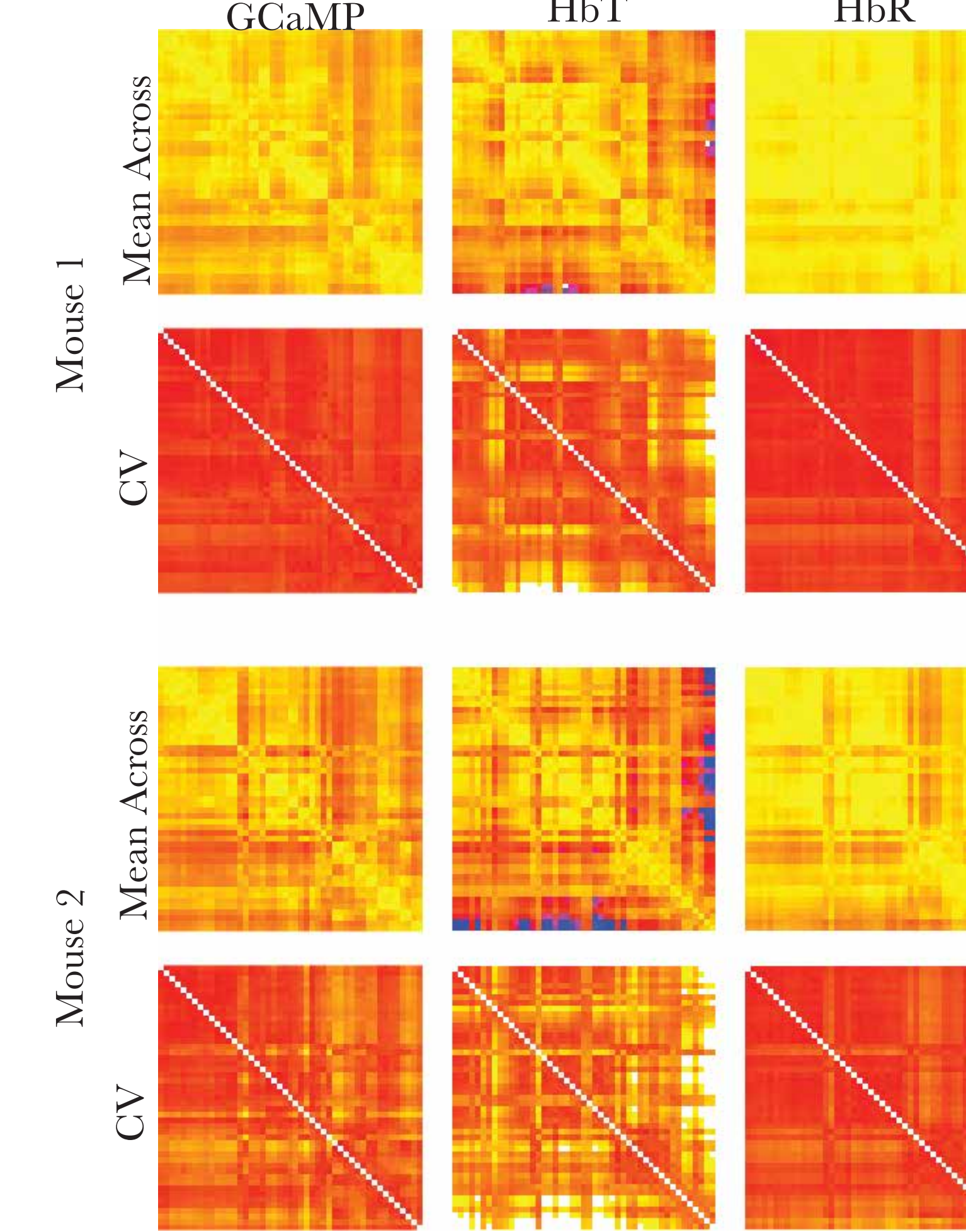
- Hutchison, et al. "Dynamic functional connectivity: promise, issues, and interpretations." *NeuroImage* 80: 360-378 (2013)
- Handwerker, et al. "Periodic changes in fMRI connectivity." *NeuroImage* 63(3): 1712-1719. (2012)
- Gonzalez-Castillo, et al. "Tracking ongoing cognition in individuals using brief, whole-brain functional connectivity patterns." *Proc Natl Acad Sci U S A* 112(28): 8762-8767. (2015)
- E.M.C. Hillman, "Optical Brain Imaging In-vivo: Techniques and Applications from Animal to Man" [Review] *J Biomed Opt.* 12(5), 051402 (2007).
- Chen, Tsai-Wen, et al. "Ultrasensitive fluorescent proteins for imaging neuronal activity." *Nature* 499.7458 295-300. (2013)
- Ma, Ying, et al. "Wide-field optical mapping of neural activity and brain haemodynamics: considerations and novel approaches." *Phil. Trans. R. Soc. B* 371.1.705 (2016); 20150360.
- Ma, Ying, et al. "Resting-state hemodynamics are spatiotemporally coupled to synchronized and symmetric neural activity in excitatory neurons." *Proceedings of the National Academy of Sciences.*
- Gonzalez-Castillo, et al. "The spatial structure of resting state connectivity stability on the scale of minutes." *Front Neurosci* 8: 138 (2014)

Correlations Across Runs

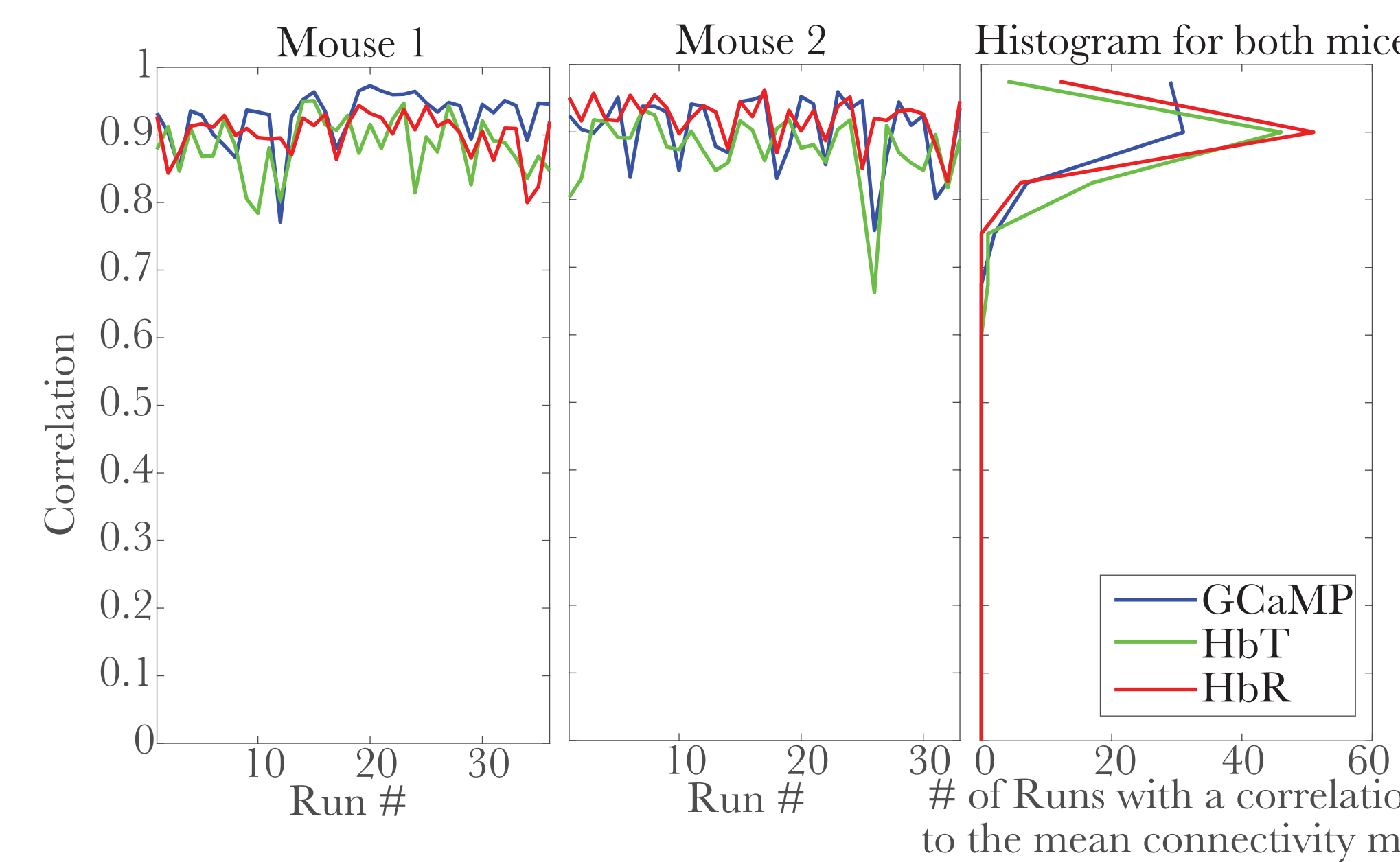
GCaMP & HbT GCaMP & HbR



Mean & Coefficient of Variation of Correlation Matrices Across Runs

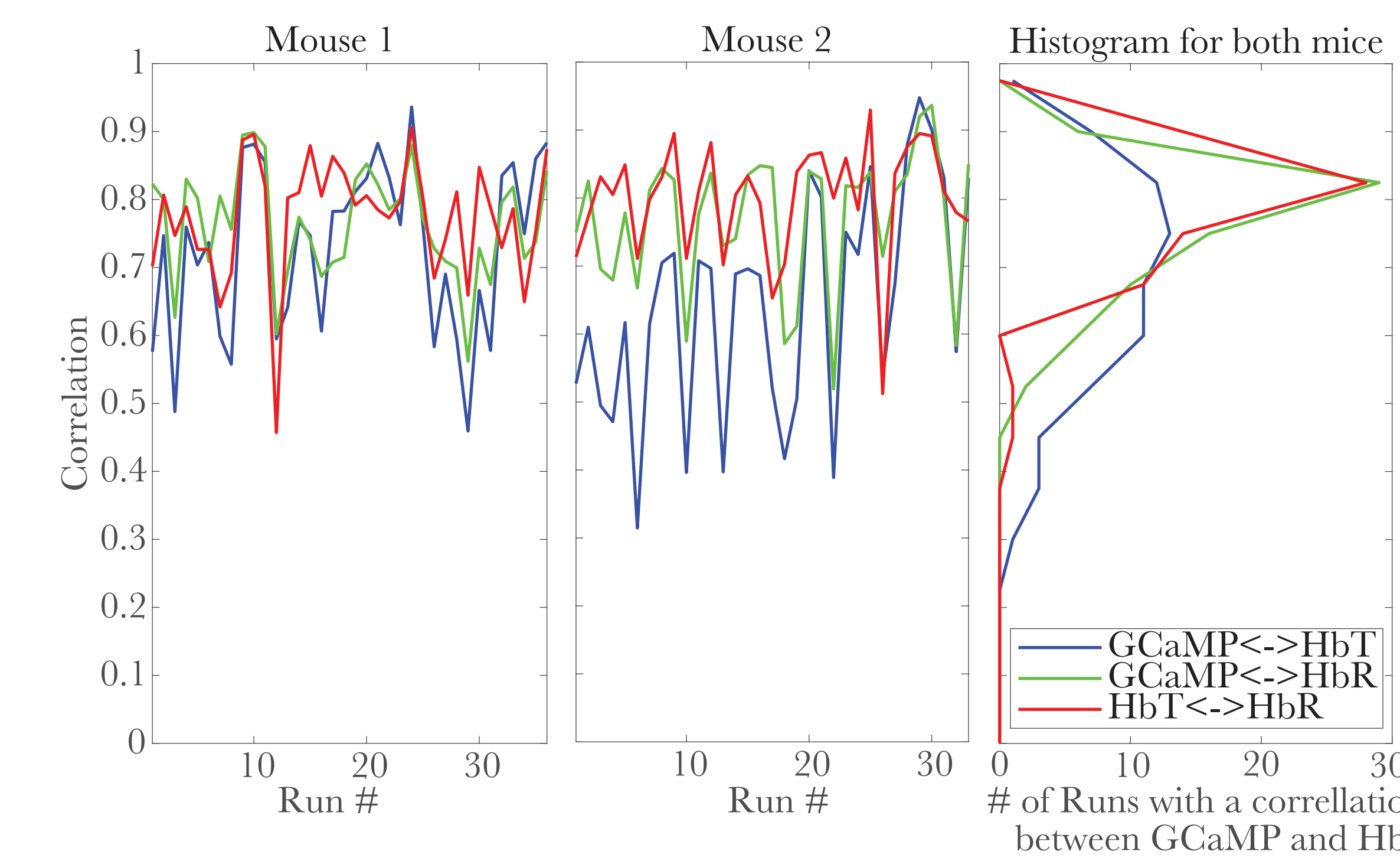


Similarity to mean connectivity map for each data source



For each data source, the mean connectivity matrix was correlated to the connectivity matrices for each run for each mouse. Larger values means the spatial pattern of the connectivity patterns are more similar. The connectivity patterns are very consistent across runs for both GCaMP and Hb measures.

Correlation between connectivity maps between data sources



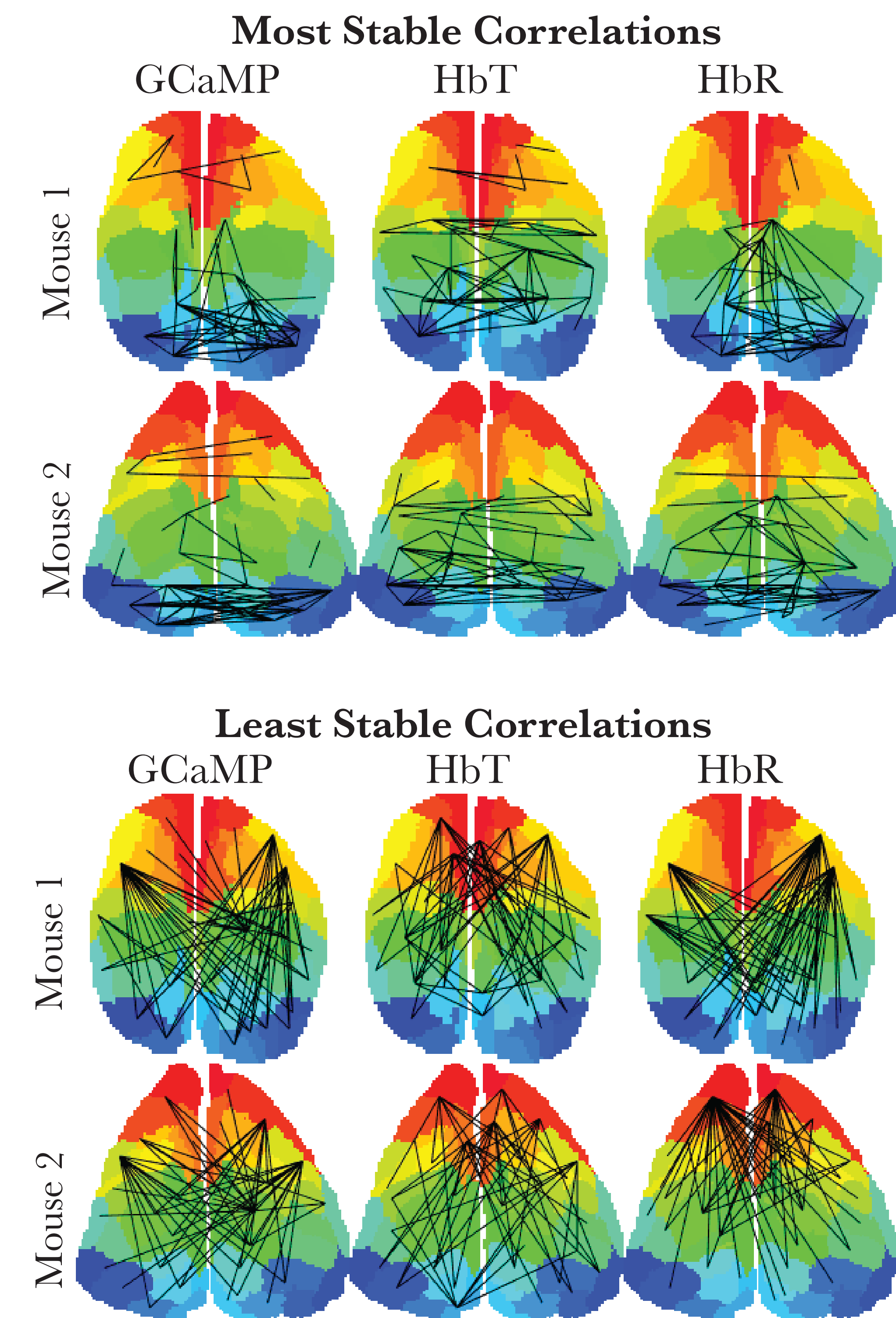
For each run, the connectivity map for one data source was correlated to the map from another data source. This highlights how similar the spatial connectivity pattern is between GCaMP and the Hb measures. These correlations are high in nearly every run, but there is more variation in the correlation magnitudes within run across modalities than across runs within a modality. The relationship between GCaMP and HbT has particularly more variability, especially in mouse 2.

RESULTS

Stability of Correlations Across Runs

For each mouse, the connectivity matrices across runs were averaged together for each data source. The average correlations for all pairs of ROIs were high. While the magnitude of the correlations varied by mouse and data source, the overall structure is visually similar. There are separation in correlation strength between more rostral and caudal ROIs.

The CV (mean/standard deviation) was calculated for all pairs of ROIs with a mean correlation > 0.1. The CVs were relatively low, meaning there was a high degree of similarity across runs, but there was variation, particularly when using the HbT data.



The 5% of connections with the highest or lowest coefficients of variation are shown. As with past work in humans, bilateral symmetric connections are the most stable [8]. The greatest stability was between visual areas. The least stable connections were between caudal areas and the rest of the brain

CONCLUSIONS

We adapt human fMRI-style connectivity analyses to mouse wide field optical mapping data

Our findings show more stability across runs than in fMRI, but there are some dynamic connectivity changes with bilateral symmetric connections being the most stable.

The connectivity maps derived from GCaMP and Hb are very similar, but not identical and the magnitude of the differences varies across runs.

Acknowledgements

NIMH Intramural Research Program
NIH Grants: RF1-MH114276, R01-NS076628, R01-NS063226, U19-NS104649, 5U01NS094296, F30-HL128023
DOD Grant (MURI, W911NF-12-1-0594)
Columbia RISE program
Simons Foundation Collaboration on the Global Brain
Kavli Foundation
This work utilized the computational resources of the NIH HPC Biowulf cluster (hpc.nih.gov)
Dylan Nielson, John Rodgers Lee, Bob Cox, Paul Taylor, Pete Molfese, Laurentius Huber, Emily Finn helped discuss aspects of these analyses